PHYSICAL REVIEW D VOLUME 22, NUMBER 3 1 AUGUST 1980

Large-P_T reactions in broken color gauge theory

Chueng Ryong Ji, Jae Kwan Kim, and Hyun Jong Shin
Department of Basic Science, Korea Advanced Institute of Science, Seoul, Korea
(Received 17 August 1979)

The lowest-order diagrams for the process of inclusive hadron production in hadron-hadron collisions are calculated in broken color symmetry. The simple comparison with the experimental data of the $pp \to \pi X$ process shows that the theoretical calculations are consistent with the data.

I. INTRODUCTION

During the last few years, perturbative calculations including strong interactions have been carried out by many people in quantum chromodynamics (QCD).[1] Their basic ingredients are the small coupling constant of the asymptotic-freedom property and the factorization property by which the mass singularity of the higher-order diagrams can be absorbed into the experimental parton distribution functions.[2] The comparison of the above various calculations with the experiments have indicated that this kind of perturbative calculation for the strong interactions is reasonably reliable. The typical example is the process such as $pp \to \pi X$. However, it has been found that nonperturbative effects such as the transverse momentum of the partons are necessary in QCD to explain the present data covering the range $19.4 \leq \sqrt{s} \leq 62.4$ GeV and $3 \leq P_T \leq 8$ GeV/c.[3] The magnitudes of the transverse momenta used in the QCD calculation for the dilepton production[4] and π production in p-p collisions[3] do not seem consistent with each other. Therefore, it will be interesting to investigate these processes in some other gauge models.

Another model for strong-interaction physics is the Pati-Salam model where color symmetry is spontaneously broken but the asymptotic-freedom property is shown to be preserved.[5] Using this model, many processes such as Compton scattering, dilepton production, and electroproduction have been analyzed successfully.[6] In this paper, we calculate the cross section of $pp \to \pi X$ in the Pati-Salam model and make a simple comparison with the experimental data. In Sec. II, we calculate the cross sections of quark-quark, quark-gluon, and gluon-gluon scattering for the massive gluons explicitly. Section III is a simple comparison of the above calculations with the experimental data to test the theoretical calculations.

II. THEORETICAL CALCULATIONS

In the broken color gauge theory, the lowest-order diagrams for the $pp \to \pi X$ process are shown in Figs. 1–5. We use the R_ξ gauge with $\xi = 0$ to remove the contribution of the ghost particles.[7] In the Pati-Salam model, the glouns mix with the weak-interaction gauge bosons by the Higgs mechanism. The magnitude of the mixing is typically an order of g/f, where g is the weak-interaction coupling constant and f is the strong-interaction coupling constant. So the mixing effect is small and it contributes negligibly. The main difference from the QCD results from the gluon mass which is obtained from the Higgs mechanism. Because of the finite gluon mass, the initial- and final-spin sums differ from the QCD case. Therefore, the calculations of the subsections, A and B, in which the gluons are not included in the external legs, are almost equal to the QCD case.[8]

A. $qq \to qq$ and $\bar{q}\bar{q} \to \bar{q}\bar{q}$

Using the Feynman diagrams in Fig. 1, the t- and u-channel amplitudes are given by

$$\mathfrak{M}_t(q^i_\alpha q^k_\beta \to q^j_\alpha q^l_\beta) = \frac{g^2}{(t-m^2)} (T^a_{ij} T^a_{kl}) \bar{u}^j_\alpha(p_4) \gamma_\mu u^i_\alpha(p_1) \times \bar{u}^l_\beta(p_3) \gamma^\mu u^k_\beta(p_2) \tag{1}$$

and

$$\mathfrak{M}_u(q^i_\alpha q^k_\beta \to q^j_\alpha q^l_\beta) = -\frac{g^2}{(u-m^2)} \delta_{\alpha\beta} (T^b_{il} T^b_{kj}) \bar{u}^j_\alpha(p_4) \gamma_\nu u^k_\beta(p_2) \times \bar{u}^l_\beta(p_3) \gamma^\nu u^i_\alpha(p_1)\,, \tag{2}$$

where T^a are $\frac{1}{2}$ times the SU(3) matrices, and m

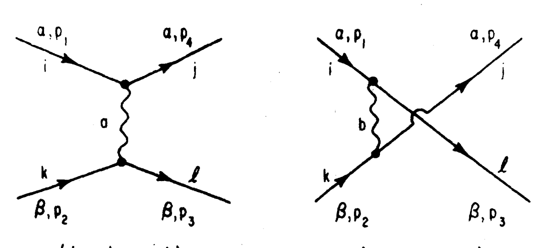

FIG. 1. Feynman diagrams for the $qq \to qq$ and $\bar{q}\bar{q} \to \bar{q}\bar{q}$ processes. The quark colors are indicated by i, j, k, and l, while the gluon colors are indicated by a and b. Also, α and β represent the quark flavors.

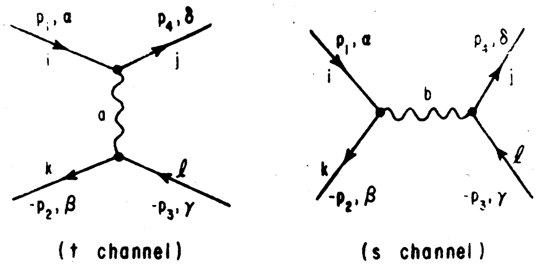

FIG. 2. Feynman diagrams for the $q\bar{q}\to q\bar{q}$ process. Indices are defined the same as in Fig. 1.

is the gluon mass.

Averaging over the initial states of the spin and the color and summing over the final states give

$$\langle|\mathfrak{M}(q_\alpha q_\beta \to q_\alpha q_\beta)|^2\rangle = g^4\left\langle\frac{2}{9}\right\rangle\left[\frac{2(s^2+u^2)}{(t-m^2)^2}+\delta_{\alpha\beta}\frac{2(t^2+s^2)}{(u-m^2)^2}+\delta_{\alpha\beta}\left\langle-\frac{1}{3}\right\rangle\frac{4s^2}{(t-m^2)(u-m^2)}\right], \tag{3}$$

where $\mathfrak{M}=\mathfrak{M}_t+\mathfrak{M}_u$. The factors which are the result of the color averages are inclosed in the angular brackets on the right side.

Because of time-reversal invariance,

$$\langle|\mathfrak{M}(\bar{q}_\alpha\bar{q}_\beta \to \bar{q}_\alpha\bar{q}_\beta)|^2\rangle = \langle|\mathfrak{M}(q_\alpha q_\beta \to q_\alpha q_\beta)|^2\rangle\,. \tag{4}$$

B. $q\bar{q}\to q\bar{q}$

The t-channel and s-channel amplitudes of this process shown in Fig. 2 are

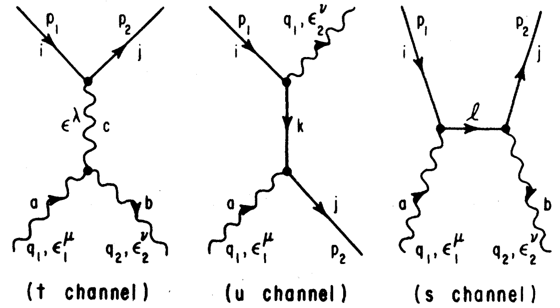

FIG. 3. Feynman diagrams for the $qg\to qg$ and $\bar{q}g\to \bar{q}g$ processes. Indices are defined the same as in Fig. 1. In addition, μ, ν, and λ represent the Lorentz indices.

$$\mathfrak{M}_t(q^i_\alpha \bar{q}^k_\beta \to q^j_\delta \bar{q}^l_\gamma) = \frac{g^2}{(t-m^2)}\,\delta_{\alpha\delta}\delta_{\beta\gamma}T^a_{ij}T^a_{lk}\bar{u}^j_\delta(p_4)\gamma_\mu u^i_\alpha(p_1) \times \bar{v}^k_\beta(p_2)\gamma^\mu v^l_\gamma(p_3) \tag{5}$$

and

$$\mathfrak{M}_s(q^i_\alpha \bar{q}^k_\beta \to q^j_\delta \bar{q}^l_\gamma) = -\frac{g^2}{(s-m^2)}\,\delta_{\alpha\beta}\delta_{\gamma\delta}T^b_{ik}T^b_{lj}\bar{u}^j_\delta(p_4)\gamma_\nu v^l_\gamma(p_3) \times \bar{v}^k_\beta(p_2)\gamma^\nu u^i_\alpha(p_1)\,. \tag{6}$$

Averaging over the initial states and summing over the final states give

$$\langle|\mathfrak{M}(q_\alpha\bar{q}_\beta \to q_\delta\bar{q}_\gamma)|^2\rangle = g^4\left\langle\frac{2}{9}\right\rangle\left[\delta_{\alpha\delta}\delta_{\beta\gamma}\frac{2(s^2+u^2)}{(t-m^2)^2}+\delta_{\alpha\beta}\delta_{\gamma\delta}\frac{2(t^2+u^2)}{(s-m^2)^2}+\delta_{\alpha\beta}\delta_{\beta\delta}\delta_{\delta\gamma}\left\langle-\frac{1}{3}\right\rangle\frac{4u^2}{(s-m^2)(t-m^2)}\right]. \tag{7}$$

C. $qg\to qg$ and $\bar{q}g\to\bar{q}g$

The amplitudes for the three channels shown in Fig. 3 are given in the form of

$$\mathfrak{M}_v(q_i g_a \to q_j g_b) = T^{\mu\nu}_v \epsilon_{1\mu}\epsilon_{2\nu}\,, \tag{8}$$

where v represents the channel. If we define

$$C^{\lambda\mu\nu}(p,q,r) = (p-q)^\nu g^{\lambda\mu} + (q-r)^\lambda g^{\mu\nu} + (r-p)^\mu g^{\nu\lambda}$$

and

f_{abc} as $[T^a, T^b] = if_{abc}T^c$,

we get

$$T^{\mu\nu}_t = \frac{g^2}{(t-m^2)} f_{cab}T^c_{ij}C^{\lambda\mu\nu}(q_1-q_2, -q_1, q_2) \times \bar{u}_j(p_2)\gamma_\lambda u_i(p_1)\,, \tag{9}$$

$$T^{\mu\nu}_u = -\frac{ig^2}{u}(T^bT^a)_{ij}\bar{u}_j(p_2)\gamma^\mu(\not{p}_1-\not{q}_2)\gamma^\nu u_i(p_1)\,, \tag{10}$$

and

$$T^{\mu\nu}_s = -\frac{ig^2}{s}(T^aT^b)_{ij}\bar{u}_j(p_2)\gamma^\nu(\not{p}_1+\not{q}_1)\gamma^\mu u_i(p_1). \tag{11}$$

From these, one can easily show that

$$T^{\mu\nu}\epsilon_{1\mu}q_{2\nu}=0\,, \tag{12}$$

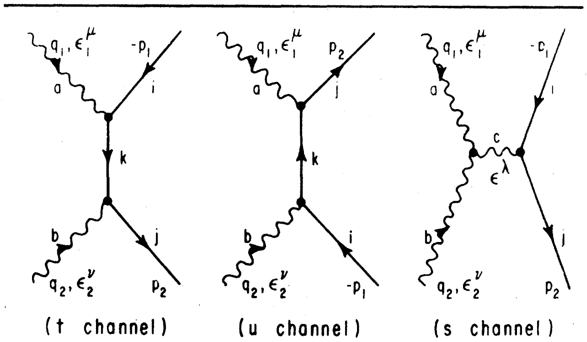

FIG. 4. Feynman diagrams for the $gg\to q\bar{q}$ and $q\bar{q}\to gg$ processes. Indices are defined the same as in Fig. 3.

where $T^{\mu\nu}=T_t^{\mu\nu}+T_s^{\mu\nu}+T_u^{\mu\nu}$.

By averaging over the initial states, summing over the final states, and using the polarization sum of the gluons,

$$\sum_{\rm pol}\epsilon^{\mu}(p)\epsilon^{\nu}(p)=-g^{\mu\nu}+\frac{p^{\mu}p^{\nu}}{m^2}\,, \tag{13}$$

we get

$$\langle|\mathfrak{M}(qg\to qg)|^2\rangle=\tfrac{1}{6}\left(\langle T^*_{\mu\nu}T^{\mu\nu}\rangle-\frac{1}{m^4}\langle|T_{\mu\nu}q_1^{\mu}q_2^{\nu}|^2\rangle\right), \tag{14}$$

where the angular brackets of the right-hand side mean the color average.

The first term of the right-hand side of formula (14) is given by

$$\begin{aligned}\langle T^*_{\mu\nu}T^{\mu\nu}\rangle&=\langle T^*_{t,\mu\nu}T_t^{\mu\nu}\rangle+\langle T^*_{u,\mu\nu}T_u^{\mu\nu}\rangle+\langle T^*_{s,\mu\nu}T_s^{\mu\nu}\rangle+\langle 2T^*_{t,\mu\nu}T_u^{\mu\nu}\rangle+\langle 2T^*_{s,\mu\nu}T_t^{\mu\nu}\rangle+\langle 2T^*_{u,\mu\nu}T_s^{\mu\nu}\rangle\\&=4g^4\left[\frac{1}{(t-m^2)^2}\left\langle\frac{1}{2}\right\rangle[4t^2+7m^2t-5(s-m^2)(u-m^2)]+\frac{1}{u^2}\left\langle\frac{2}{9}\right\rangle(-2su+6m^4)\right.\\&\quad+\frac{1}{s^2}\left\langle\frac{2}{9}\right\rangle(-2us+6m^4)+\left\langle\frac{i}{4}\right\rangle\frac{4i}{(t-m^2)u}[-(u-m^2)^2-2m^2t]\\&\quad\left.+\left\langle-\frac{i}{4}\right\rangle\frac{-4i}{(t-m^2)s}[-(s-m^2)^2-2m^2t]+\left\langle-\frac{1}{36}\right\rangle\frac{-8m^2t}{su}\right],\end{aligned} \tag{15}$$

and the second term of the right-hand side of the formula (14) is given by

$$\begin{aligned}&\frac{1}{m^4}\langle|T_{\mu\nu}q_1^{\mu}q_2^{\nu}|^2\rangle\\&\quad=4g^4\frac{1}{(t-m^2)^2}\left\langle\frac{1}{2}\right\rangle\left[-\frac{(s-m^2)(u-m^2)}{2}+\frac{m^2}{2}t\right].\end{aligned} \tag{16}$$

Because of time-reversal invariance,

$$\langle|\mathfrak{M}(\bar{q}g\to\bar{q}g)|^2\rangle=\langle|\mathfrak{M}(qg\to qg)|^2\rangle. \tag{17}$$

D. $gg\to q\bar{q}$ and $q\bar{q}\to gg$

These processes shown in Fig. 4 can be obtained from the $qg\to qg$ process by crossing and are given by

$$\langle|\mathfrak{M}(gg\to q\bar{q};s,t,u)|^2\rangle=-\tfrac{1}{4}\langle|\mathfrak{M}(qg\to qg;t,s,u)|^2\rangle, \tag{18}$$

and from time-reversal invariance,

$$\langle|\mathfrak{M}(q\bar{q}\to gg)|^2\rangle=16\,\langle|\mathfrak{M}(gg\to q\bar{q})|^2\rangle. \tag{19}$$

E. $gg\to gg$

As in the case of the subsection C, the amplitude of this process shown in Fig. 5 has the form

$$\mathfrak{M}_v(gg\to gg)=T_v^{\lambda\mu\nu\sigma}\epsilon_{1\lambda}\epsilon_{2\mu}\epsilon_{3\nu}\epsilon_{4\sigma}\,, \tag{20}$$

where v represents the channel.

$T_v^{\lambda\mu\nu\sigma}$'s are given for the value of $v=t,u,s,4$ as

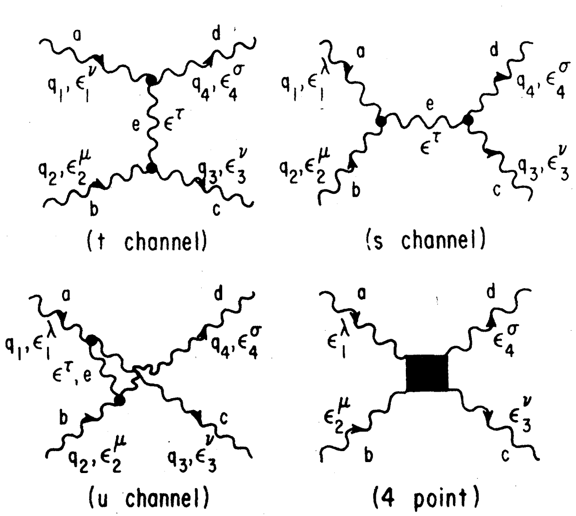

FIG. 5. Feynman diagrams for the $gg\to gg$ process. Indices are defined the same as in Fig. 3.

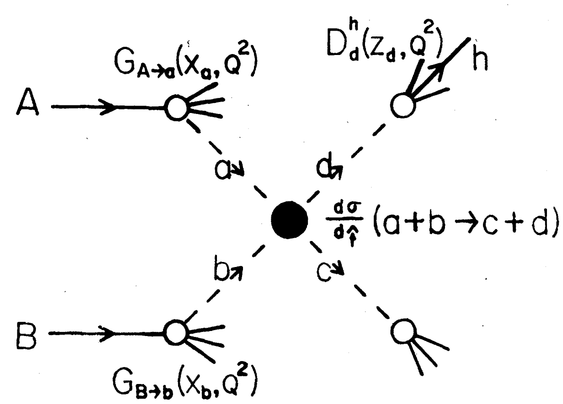

FIG. 6. Illustration of the $A+B\to h+X$ process. $G_{A\to a}(x_a,Q^2)$ $[G_{B\to b}(x_b,Q^2)]$ is the distribution function of the parton a $[b]$ in the hadron A $[B]$, and $D_d^h(z_d,Q^2)$ is the fragmentation function of the parton d into the hadron h. $(d\sigma/d\hat{t})$ $(a+b\to c+d)$ is the differential cross section of the parton-parton scattering. The kinematical variables of the hadrons (partons) are s, t, and u ($\hat{s}$, $\hat{t}$, and $\hat{u}$).

follows:

$$T_t^{\lambda\mu\nu\sigma}=-ig^2 f_{aed} f_{ebc} C^{\lambda\tau\sigma}(-q_1, q_1-q_4, q_4)\times\left(\frac{g_{\tau\tau'}-k_\tau k_{\tau'}/m^2}{t-m^2}\right)C^{\tau'\mu\nu}(q_2-q_3,-q_2,q_3)\,, \tag{21}$$

where $k=q_1-q_4$;

$$T_u^{\lambda\mu\nu\sigma}=-ig^2 f_{aec} f_{ebd} C^{\lambda\tau\nu}(-q_1, q_1-q_3, q_3)\times\left(\frac{g_{\tau\tau'}-k_\tau k_{\tau'}/m^2}{u-m^2}\right)C^{\tau'\mu\sigma}(q_2-q_4,-q_2,q_4), \tag{22}$$

where $k=q_1-q_3$;

$$T_s^{\lambda\mu\nu\sigma}=-ig^2 f_{abe} f_{ecd} C^{\lambda\mu\tau}(-q_1,-q_2, q_1+q_2)\times\left(\frac{g_{\tau\tau'}-k_\tau k_{\tau'}/m^2}{s-m^2}\right)C^{\tau'\nu\sigma}(-q_3-q_4,q_3,q_4), \tag{23}$$

where $k=q_1+q_2$;

$$T_4^{\lambda\mu\nu\sigma}=-ig^2[f_{abe}f_{cde}(g^{\lambda\nu}g^{\mu\sigma}-g^{\lambda\sigma}g^{\mu\nu})+f_{ace}f_{bde}(g^{\lambda\mu}g^{\nu\sigma}-g^{\lambda\sigma}g^{\nu\mu})+f_{ade}f_{cbe}(g^{\lambda\nu}g^{\mu\sigma}-g^{\lambda\mu}g^{\sigma\nu})]\,. \tag{24}$$

As we show in the Appendix,

$$T^{\lambda\mu\nu\sigma}q_{1\lambda}\epsilon_{2\mu}\epsilon_{3\nu}\epsilon_{4\sigma}=0\,, \tag{25}$$

where

$$T^{\lambda\mu\nu\sigma}=T_t^{\lambda\mu\nu\sigma}+T_u^{\lambda\mu\nu\sigma}+T_s^{\lambda\mu\nu\sigma}+T_4^{\lambda\mu\nu\sigma}\,.$$

Thus, when we square the amplitudes and sum over the final states and average over the initial states, we get

$$\begin{aligned}\langle|\mathfrak{M}(gg\to gg)|^2\rangle=\tfrac{1}{9}\Big[&\langle T^*_{\lambda\mu\nu\sigma}T^{\lambda\mu\nu\sigma}\rangle-\frac{1}{m^4}(\langle|T_{\lambda\mu\nu\sigma}q_1^\lambda q_2^\mu\epsilon_3^\nu\epsilon_4^\sigma|^2\rangle+\langle|T_{\lambda\mu\nu\sigma}q_1^\lambda\epsilon_2^\mu q_3^\nu\epsilon_4^\sigma|^2\rangle\\&+\langle|T_{\lambda\mu\nu\sigma}q_1^\lambda\epsilon_2^\mu\epsilon_3^\nu q_4^\sigma|^2\rangle+\langle|T_{\lambda\mu\nu\sigma}\epsilon_1^\lambda q_2^\mu q_3^\nu\epsilon_4^\sigma|^2\rangle+\langle|T_{\lambda\mu\nu\sigma}\epsilon_1^\lambda q_2^\mu\epsilon_3^\nu q_4^\sigma|^2\rangle\\&+\langle|T_{\lambda\mu\nu\sigma}\epsilon_1^\lambda\epsilon_2^\mu q_3^\nu q_4^\sigma|^2\rangle)+\frac{1}{m^6}(\langle|T_{\lambda\mu\nu\sigma}q_1^\lambda q_2^\mu q_3^\nu\epsilon_4^\sigma|^2\rangle+\text{permutations})\\&-\frac{1}{m^8}\langle|T_{\lambda\mu\nu\sigma}q_1^\lambda q_2^\mu q_3^\nu q_4^\sigma|^2\rangle\Big]\,.\end{aligned} \tag{26}$$

The first term of the right-hand side of the formula (26) is calculated as

$$\begin{aligned}\langle T^*_{\lambda\mu\nu\sigma}T^{\lambda\mu\nu\sigma}\rangle&=\langle T^*_{t,\lambda\mu\nu\sigma}T_t^{\lambda\mu\nu\sigma}\rangle+\langle t\leftrightarrow u\rangle+\langle t\leftrightarrow s\rangle+\langle T^*_{4,\lambda\mu\nu\sigma}T_4^{\lambda\mu\nu\sigma}\rangle+\langle 2T^*_{t,\lambda\mu\nu\sigma}T_u^{\lambda\mu\nu\sigma}\rangle+\langle u\leftrightarrow s\rangle\\&\quad+\langle t\leftrightarrow s\rangle+\langle 2T^*_{4,\lambda\mu\nu\sigma}(T_t^{\lambda\mu\nu\sigma}+T_u^{\lambda\mu\nu\sigma}+T_s^{\lambda\mu\nu\sigma})\rangle\\&=g^4\Big[\left\langle\frac{9}{8}\right\rangle\bigg(\Big\{\frac{1}{(t-m^2)^2}[(4t+2m^2)(2t+28m^2)+\tfrac{53}{2}(t+2m^2)^2-25(s-2m^2)(u-2m^2)]\Big\}\\&\quad+\{t\leftrightarrow u\}+\{t\leftrightarrow s\}\bigg)+\langle\tfrac{9}{8}\rangle(108)\\&\quad+2\left\langle\frac{9}{16}\right\rangle\Big\{\Big[\Big(30-\frac{3}{2}\frac{s^2}{tu}\Big)+6m^2\frac{s}{tu}\Big(5+9\frac{m^2}{s}\Big)\Big]+[u\leftrightarrow s]+[t\leftrightarrow s]\Big\}+3\langle\tfrac{9}{8}\rangle(-81)\Big]\,.\end{aligned} \tag{27}$$

The term containing $1/m^4$ in formula (26) is calculated as

$$\begin{aligned}&-\frac{1}{m^4}(\langle|T_{\lambda\mu\nu\sigma}q_1^\lambda q_2^\mu\epsilon_3^\nu\epsilon_4^\sigma|^2\rangle+\text{permutations})\\&=-2g^4\Big[\left\langle\frac{9}{8}\right\rangle\bigg(\Big\{\frac{1}{(s-m^2)^2}\Big[12m^4-2sm^2+(\tfrac{7}{4}s^2-3tu)+(tu-\tfrac{5}{4}s^2)\frac{s}{m^2}+\Big(\tfrac{3}{16}s^2-\frac{tu}{4}\Big)\frac{s^2}{m^4}\Big]\Big\}+\{s\leftrightarrow t\}+\{s\leftrightarrow u\}\bigg)\\&\quad+2\left\langle\frac{9}{16}\right\rangle\bigg(\Big\{\frac{1}{(s-m^2)(t-m^2)}\Big[-2um^2+\Big(\frac{3}{2}u^2+\frac{st}{2}\Big)+\Big(-\frac{u^2}{4}+\frac{7}{8}st\Big)\frac{u}{m^2}+\Big(\frac{3}{16}st-\frac{u^2}{8}\Big)\frac{st}{m^4}\Big]\Big\}\\&\quad+\{t\leftrightarrow u\}+\{s\leftrightarrow u\}\bigg)\Big]\,.\end{aligned} \tag{28}$$

The term containing $1/m^6$ in formula (26) is calculated as

$$\frac{1}{m^6}\left(\langle|T_{\lambda\mu\nu\sigma}q_1^\lambda q_2^\mu q_3^\nu \epsilon_4^\sigma|^2\rangle + \text{permutations}\right) = 2g^4\left\{\left\langle\frac{9}{8}\right\rangle\left[-4+\frac{(s-2m^2)^2}{2m^4}+\frac{(t-2m^2)^2}{4m^4}+\frac{(u-2m^2)^2}{4m^4}\right] + 2\left\langle\frac{9}{16}\right\rangle\left(1-\frac{s}{4m^2}\right)s\right\}$$

$$= 9g^4\left(\frac{s^2+t^2+u^2}{16m^4}-1\right). \tag{29}$$

Finally, the last term of formula (26) is calculated as

$$-\frac{1}{m^8}\langle|T_{\lambda\mu\nu\sigma}q_1^\lambda q_2^\mu q_3^\nu q_4^\sigma|^2\rangle = -\frac{g^4}{16m^4}\left(\left\langle\frac{9}{8}\right\rangle\left\{\left[\left(\frac{t}{t-m^2}\right)^2(s-u)^2\right]+[t\leftrightarrow u]+[t\leftrightarrow s]\right\} + 2\left\langle\frac{9}{16}\right\rangle\left\{\left[\left(\frac{t}{t-m^2}\right)\left(\frac{u}{u-m^2}\right)(s-u)(s-t)\right]+[u\leftrightarrow s]+[t\leftrightarrow s]\right\}\right). \tag{30}$$

Some part of the above calculations is derived using the method shown in the Appendix. As we can see easily from the nature of the process $gg \to gg$, the above formula has manifestly s, t, u symmetry.

F. Cross section

In Fig. 6 we show the process $A + B \to h + X$. If one neglects the masses of the partons, one can derive the simple relation between the differential cross section of the parton-parton scattering and the square of the invariant amplitude as

$$\frac{d\sigma}{d\hat{t}}(a+b\to c+d) = \frac{1}{16\pi\hat{s}^2}\langle|\mathfrak{M}(a+b\to c+d;\hat{s}+\hat{t}+\hat{u}=0)|^2\rangle. \tag{31}$$

Also the invariant cross section corresponding to Fig. 6 can be related to the above differential cross section of the parton-parton scattering as

$$E\frac{d\sigma}{d^3p}(A+B\to h+X) = \int_{x_a^{\min}}^1 dx_a \int_{x_b^{\min}}^1 dx_b G_{A\to a}(x_a,Q^2) G_{B\to b}(x_b,Q^2) D_d^h(z_d,Q^2)\frac{1}{z_d\pi}\frac{d\sigma}{d\hat{t}}(a+b\to c+d), \tag{32}$$

where

$$x_a^{\min} = -\frac{u}{s+t},\quad x_b^{\min} = -\frac{x_a t}{x_a s + u},\quad z_d = -\frac{x_a t + x_b y}{x_a x_b s}$$

from the constraints of

$$0 \leq x_a \leq 1,\quad 0 \leq x_0 \leq 1,\quad 0 \leq z_d \leq 1,$$

and $s + t + u = 0$.

III. SIMPLE COMPARISON WITH EXPERIMENT

The detailed analysis of the large-P_T reactions using the QCD calculations have been carried out several times by now. In this paper, we want to see the simple consequence of the above calculations in the Pati-Salam model following the method of the QCD. In order to calculate the cross section of $pp \to \pi X$, one must know the momentum distributions of the gluons and the quarks within the proton and the probability distributions for a scattered gluon or quark to produce a hadron. As the structures of the Pati-Salam model and the QCD are almost the same, the parton distribution functions or the fragmentation functions of the Pati-Salam model are approximately equal to the QCD. We use the Buras-Gaemer[9] parametrization for the parton distribution function. For the fragmentation function, the parametrization determined by Owens, Reya, and Glück[10] is used.

In Fig. 7, our calculations for high-p_T inclusive pion production are compared with the data for $\sqrt{s} = 52.7$ and 62.4 GeV and $2 \leq P_T \leq 11$ GeV/c. The agreement between the calculation of the Pati-Salam model and the experimental data is not so bad even without including the intrinsic transverse momentum of the parton. In the above fitting the only parameter is the effective gluon mass and it is found to be around 0.3 GeV. However, the inclusion of the intrinsic transverse momenta of the partons will improve the agreement between the model calculations and experimental data. In addition, this inclusion will change somewhat the effective mass of the gluons.

At this point, it is important to discuss the main differences between the predictions from the present model and the standard QCD. Figure 7 clearly exhibits that the present model gives a more steeply rising cross section at the smaller-P_T region than QCD. In Fig. 8, we show the calculations for the separate contributions of the three major subprocesses at $\sqrt{s} = 62.4$ GeV. At the low-P_T region the gluon-gluon subprocess dominates

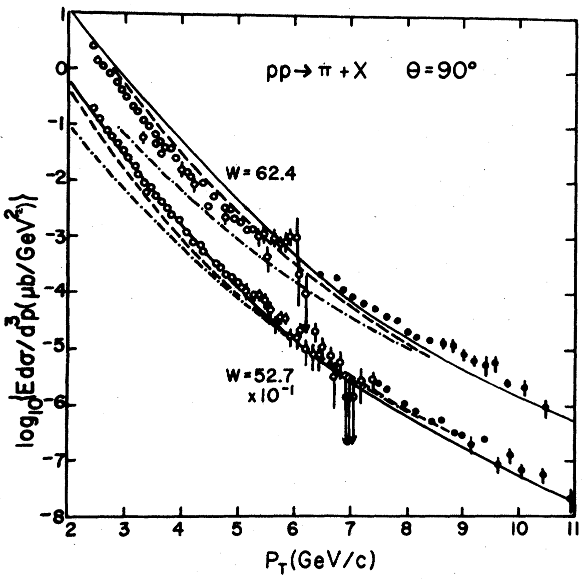

FIG. 7. Comparison of the Pati-Salam model without the intrinsic transverse momentum with the data on the high-P_T pion production in the proton-proton collision for $W=\sqrt{s}=62.4$ and 53 GeV with $\theta=90°$ in the c.m. system (open circle: Ref. 11, solid dots: Ref. 12). The solid curves show the results of the Pati-Salam model calculations. The dashed and dot-dashed curves show the results of the QCD with and without the intrinsic transverse momentum (Owens and Kimel, and Feynman, Field, and Fox in Ref. 3).

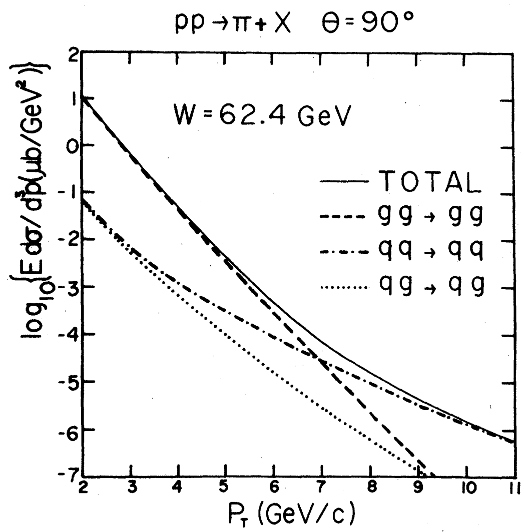

FIG. 8. Individual contributions of the three major subprocesses to the solid curve for $W=62.4$ GeV in Fig. 7.

while for the large-P_T region the quark-quark subprocess is more important. Thus, the steeper rise in the cross section at the smaller-P_T region comes from the gluon-gluon subprocess which is most different from the QCD.

The above differences in the gluon-gluon subprocess can be caused by the extra polarization states of the glue and by the extra explicit kinematic mass dependence compared to the unbroken theory. Owing to the extra polarization state in the present model, the polarization average factor in our case is $\frac{1}{9}$ rather than $\frac{1}{4}$ in the case of QCD and also the formula (13) for the polarization sum in our case is different from that of the QCD of of the massless gluon. The $p^\mu p^\nu/m^2$ term in the formula (13), which is typical for the massive gluon theory, leads to the gluon mass dependence in formulas (28)–(30) of the gluon-gluon subprocess. As we see in those formulas, they become large as the gluon mass m becomes small and even diverge at $m=0$. Owing to this strong gluon-mass dependence in formulas (28)–(30), the invariant amplitude of our gluon-gluon subprocess with our choice of gluon mass 0.3 GeV/c is much larger than that of the QCD in spite of the smallness of the polarization average factor. The other differences due to the extra explicit gluon-mass dependence such as in the gluon propagator or in the kinematic incident-flux factor are negligible in the energy range of this high-P_T experiment.

For the relatively-large-P_T region, the main contribution to the cross section comes from the quark-quark subprocess. The only difference in our calculation of this subprocess with respect to the QCD is the extra explicit gluon mass dependence which is negligible as in the calculation of the gluon-gluon subprocess. So in the larger-P_T region, our prediction is almost equal to that of the QCD.

A detailed analysis including all available experimental data for all energy regions and the intrinsic transverse momentum of the partons will be necessary to make a careful comparison between the Pati-Salam model and QCD.

ACKNOWLEDGMENT

This research was supported by Korea Research Center for Theoretical Physics and Chemistry and by KOSEF-NSF cooperative research program.

APPENDIX

Here we show explicitly the calculation of formula (25). By substituting $q_{4\sigma}$ instead of $\epsilon_{4\sigma}$ in the invariant amplitudes given by formulas (21)–(24), we simply write the following:

$$T_t^{\lambda\mu\nu\sigma}\epsilon_{1\lambda}\epsilon_{2\mu}\epsilon_{3\nu}q_{4\sigma}=-ig^2 f_{aed}f_{ebc}\Big[\frac{1}{(t-m^2)}\{(t-m^2)(2q_2\cdot\epsilon_3\epsilon_2\cdot\epsilon_1-q_2\cdot\epsilon_1\epsilon_2\cdot\epsilon_3+2q_3\cdot\epsilon_2\epsilon_3\cdot\epsilon_1$$
$$-q_3\cdot\epsilon_3\epsilon_2\cdot\epsilon_1-q_2\cdot\epsilon_2\epsilon_3\cdot\epsilon_1-q_3\cdot\epsilon_1\epsilon_2\cdot\epsilon_3)$$
$$-q_1\cdot\epsilon_1[(q_2+q_3)\cdot q_4\epsilon_2\cdot\epsilon_3+(2q_2-q_3)\cdot\epsilon_3(-q_4\cdot\epsilon_2)+2(q_3-q_2)\cdot\epsilon_2(-q_4\cdot\epsilon_3)]$$
$$+q_2\cdot\epsilon_2(-q_4\cdot\epsilon_1q_2\cdot\epsilon_3)+q_3\cdot\epsilon_3(q_4\cdot\epsilon_1q_3\cdot\epsilon_2)\}\Big],\qquad\text{(A1)}$$

$$T_s^{\lambda\mu\nu\sigma}\epsilon_{1\lambda}\epsilon_{2\mu}\epsilon_{3\nu}q_{4\sigma}=-ig^2 f_{abe}f_{ecd}[(t\leftrightarrow s,\ \ q_3\leftrightarrow -q_1,\ \ \epsilon_4\leftrightarrow\epsilon_1)\ \text{ in (A1)}],\qquad\text{(A2)}$$

$$T_u^{\lambda\mu\nu\sigma}\epsilon_{1\lambda}\epsilon_{2\mu}\epsilon_{3\nu}q_{4\sigma}=+ig^2 f_{aec}f_{ebd}[(s\leftrightarrow u,\ \ q_2\leftrightarrow -q_3,\ \ \epsilon_2\leftrightarrow\epsilon_3)\ \text{ in (A2)}],\qquad\text{(A3)}$$

$$T_4^{\lambda\mu\nu\sigma}\epsilon_{1\lambda}\epsilon_{2\mu}\epsilon_{3\nu}q_{4\sigma}=-ig^2[f_{abe}f_{cde}(\epsilon_1\cdot\epsilon_3\epsilon_2\cdot q_4-\epsilon_1\cdot q_4\epsilon_2\cdot\epsilon_3)+f_{ace}f_{bde}(\epsilon_1\cdot\epsilon_2\epsilon_3\cdot q_4-\epsilon_1\cdot q_4\epsilon_2\cdot\epsilon_3)$$
$$+f_{ade}f_{cbe}(\epsilon_1\cdot\epsilon_3\epsilon_2\cdot q_4-\epsilon_1\cdot\epsilon_2\epsilon_3\cdot q_4)].\qquad\text{(A4)}$$

The sum of the terms of Eqs. (A1)–(A3) except the terms containing the factor $q_i\cdot\epsilon_i$ $(i=1,2,3)$ are canceled out with the terms of formula (A4) using the Jacobi identity so that the remaining terms are given by

$$T_{\lambda\mu\nu\sigma}\epsilon_1^\lambda\epsilon_2^\mu\epsilon_3^\nu q_4^\sigma=-ig^2 f_{aed}f_{ebc}\Big[\Big(\frac{1}{t-m^2}\Big)\{-q_1\cdot\epsilon_1[(q_2+q_3)\cdot q_4\epsilon_2\cdot\epsilon_3+(q_3-2q_2)\cdot\epsilon_3q_4\cdot\epsilon_2+(q_2-2q_3)\cdot\epsilon_2q_4\cdot\epsilon_3]$$
$$+q_2\cdot\epsilon_2(-q_4\cdot\epsilon_1q_2\cdot\epsilon_3)+q_3\cdot\epsilon_3(q_4\cdot\epsilon_1q_3\cdot\epsilon_2)\}\Big]$$
$$-ig^2 f_{abe}f_{ecd}[(t\to s,\ \ q_3\leftrightarrow -q_1,\ \ \epsilon_3\leftrightarrow\epsilon_1)]+ig^2 f_{aec}f_{ebd}[(s\to u,\ \ q_2\leftrightarrow -q_3,\ \ \epsilon_3\leftrightarrow\epsilon_2)].\qquad\text{(A5)}$$

Using the condition of $\epsilon_i\cdot q_i=0\,(i=1,2,3,4)$, we get

$$T_{\lambda\mu\nu\sigma}\epsilon_1^\lambda\epsilon_2^\mu\epsilon_3^\nu q_4^\sigma=0\,.\qquad\text{(A6)}$$

To calculate formula (28), one can simply substitute q_i in place of ϵ_i in Eq. (A5). Likewise, the terms of Eq. (29) and Eq. (30) can be calculated by the above technique.

[1]See review by R. D. Field, in *Proceedings of the 19th International Conference on High Energy Physics, Tokyo, 1978*, edited by S. Homma, M. Kawaguchi, and H. Miyazawa (Physical Society of Japan, Tokyo, 1979), p. 743.

[2]See review by C. T. Sachrajda, in *Phenomenology of Quantum Chromodynamics*, proceedings of the XIII Rencontre De Moriond, 1978, edited by J. Trân Thanh Vân (Editions Frontières, Gif-sur-Yvette, 1978), p. 17.

[3]R. P. Feynman, R. D. Field, and G. C. Fox, Phys. Rev. D 18, 3320 (1978); R. D. Field, Phys. Rev. Lett. 40, 997 (1978); R. Cutler and D. Sivers, Phys. Rev. D 17, 196 (1977); B. L. Combridge, J. Kripfganz, and J. Ranft, Phys. Lett. 70B, 234 (1977); A. P. Contogouris, R. Gaskell, and S. Papadopoulos, Phys. Rev. D 17, 2314 (1978); J. F. Owens, E. Reya, and M. Glück, *ibid.* 18, 1501 (1978); J. F. Owens and J. D. Kimel, *ibid.* 18, 3313 (1978).

[4]G. Altarelli, G. Parisi, and R. Petronzio, Phys. Lett. 76B, 351 (1978); 76B, 356 (1978).

[5]J. C. Pati and A. Salam, Phys. Rev. D 6, 1240 (1973); Phys. Rev. Lett. 31, 661 (1973); *ibid.* 36, 1229 (1976); *ibid.* 35, 11 (1976); H. D. Politzer, Phys. Rep. C14, 129 (1974); A. Salam and J. Strathdee, Phys. Rev. D 18, 4713 (1978).

[6]H. K. Lee and J. K. Kim, Phys. Rev. Lett. 40, 485 (1978); Phys. Rev. D 18, 3985 (1978); J. K. Kim and I. G. Koh, *ibid.* 19, 1509 (1979); P. N. Pandita and S. Paranjape, Phys. Lett. 81B, 351 (1979); J. K. Kim, I. G. Koh, and H. J. Shin (unpublished).

[7]E. S. Abers and B. W. Lee, Phys. Rep. 9C, 1 (1973).

[8]R. Cutler and D. Sivers, Phys. Rev. D 17, 196 (1978).

[9]A. J. Buras and K. J. F. Gaemers, Nucl. Phys. B132, 249 (1978).

[10]J. F. Owens, E. Reya, and M. Glück, Phys. Rev. D 18, 1501 (1978).

[11]F. W. Büsser *et al.*, Nucl. Phys. B106, 1 (1976).

[12]B. G. Pope, in *Particles and Fields—1977*, proceedings of the Meeting of the Division of Particles and Fields of the APS, Argonne, Illinois, edited by P. A. Schreiner, G. H. Thomas, and A. B. Wicklund, (AIP, New York, 1978), p. 193.